Mass-selected infrared photodissociation spectroscopy of $V_4O_{10}^+$

K. R. Asmis,*[a] M. Brümmer,[a] C. Kaposta,[a] G. Santambrogio,[a] G. von Helden,[b] G. Meijer,[bc] K. Rademann[d] and L. Wöste[a]

[a] Institut für Experimentalphysik, Freie Universität Berlin, Arnimallee 14, D 14195 Berlin, Germany. E-mail: asmis@physik.fu-berlin.de; Fax: +49 30 83855567; Tel: +49 30 83856120

[b] FOM Institute for Plasma Physics Rijnhuizen, Edisonbaan 14, NL-3430 BE Nieuwegein, The Netherlands

[c] Department of Molecular and Laser Physics, University of Nijmegen, Toernooiveld, NL-6525 ED Nijmegen, The Netherlands

[d] Institut für Chemie, Humboldt Universität Berlin, Bunsenstrasse 1, D 14195 Berlin, Germany

The gas-phase infrared spectroscopy of $V_4O_{10}^+$ produced by laser vaporization has been studied in the spectral region from 7 to 16 μm. Mass-selected $V_4O_{10}^+$ cations were stored in a helium filled radio frequency hexadecapole ion trap and excited using tunable infrared radiation from a free electron laser. The photodissociation spectrum was recorded by monitoring the $V_4O_8^+$ yield (O_2 loss) as a function of the excitation wavelength. Two absorption bands at 842 and 1032 cm^{-1} are observed, which are assigned to resonant excitation of the antisymmetric V–O–V stretching and V=O stretching vibrations, respectively. Comparison to recent theoretical and experimental studies indicate that the absorbing species consists of a $V_4O_8^+$ ionic core weakly bound to an oxygen molecule.

Vanadium oxides are becoming increasingly important in technological applications, *e.g.*, as catalysts for oxidation–reduction reactions, semiconductors, optical devices and coatings.[1–3] Despite the importance of bulk V_2O_5 as a catalyst many microscopic details of its catalytic behavior remain under debate.[3] Understanding the nature of the reactive sites in heterogeneous catalysis can be aided by gas-phase studies of isolated neutral and ionic clusters. However, only scarce experimental information on the spectroscopy and structure of vanadium oxide clusters is available,[4–7] complicating the interpretation of the gas-phase reactivity studies.[8–17]

Studies of the mass spectral distributions and cluster growth dynamics of vanadium oxide clusters[18,19] and cluster ions[8,12] show that VO_2, VO_3, and V_2O_5 units are the main building blocks for $V_xO_y^{-/0/+}$ clusters. Oxygen-rich cluster ions can also contain a weakly bound O_2 species, as was shown in recent collision induced dissociation (CID) and 532 nm photofragmentation studies.[7,8] Gas phase reactivity studies indicate that the reactivity of vanadium oxide cluster anions and cations depends on cluster stoichiometry and generally decreases with cluster size.[10,13] However, with the exception of the diatomic VO (see ref. 20 and references therein), which has been found in the spectra of metal-rich M-type stars,[21] very few spectroscopic studies have been carried out on larger vanadium oxide clusters. Wu *et al.* have measured the photoelectron spectra of the vanadium oxide anions VO_x^- ($x = 1 – 4$).[4] Matrix ESR[5] and FTIR[6] studies have also been reported for monovanadium oxides and V_2O_2. Comprehensive theoretical studies on the structure, energetics and bonding of vanadium oxide clusters and cluster ions have recently been reported.[22–24]

Vibrational spectroscopy of gas phase clusters and cluster ions is a straightforward approach to probe the structure of these species. However, conventional absorption measurements, a standard tool for the characterization of liquid and solid samples, lack the sensitivity and selectivity required for studying isolated gas phase species, due mainly to the low number densities compared to the condensed systems. Therefore in recent years much effort has been put into the development of experimental methods to study the infrared (IR) spectroscopy of gas phase ions.[25,26] However, most of these studies have been limited to the wavelength region below 3 μm, *i.e.*, the spectral region of hydrogen-stretching motions and of the IR-active combination bands, due to the lack of widely tunable IR light sources. The application of a free-electron laser, which emits widely tunable light from the near to the far IR-region, to molecular spectroscopy by Meijer and coworkers has bridged this gap.[27–29]

In the present study we combine for the first time, to the best of our knowledge, tandem mass spectroscopy with a free-electron laser to study the vibrational spetroscopy of mass-selected vanadium oxide cluster ions by mass-selected IR photodissociation spectroscopy. After a brief description of the novel experimental apparatus, we present the gas phase IR photodissociation spectrum of the $V_4O_{10}^+$ cation. The results are compared to calculated IR spectra[23] of various neutral V_4O_{10} isomers and discussed with respect to structure and dissociation mechanism.

IR photodissociation spectra were obtained by photoexcitation of mass selected $V_4O_{10}^+$ and subsequent monitoring of the $V_4O_8^+$ fragment ion yield as a function of the excitation wavelength. The experiments were carried out in a novel guided ion beam tandem mass spectrometer, schematically depicted in Fig. 1, and using a widely tunable IR free electron laser.

IR excitation is performed with the "Free Electron Laser for Infrared eXperiments" (FELIX).[30] The laser output consists of a macropulse of 5 μs duration at 5 Hz. The macro pulse is composed of a series of ~1 picosecond duration micro pulses spaced by one nanosecond. The wavelength is continuously tunable between 5 and 250 μm. The bandwidth is nearly transform limited and depends on the micro pulse duration. In the present experiments the wavelength was scanned from 7.0 to 16 μm, the scanning range determined by the transmission function of the ZnSe optics used in the present experiment, in steps of 0.10 μm. Higher resolution spectra were measured with a step size of 0.02 μm in selected spectral regions. The

macro pulse energy was 50–60 mJ, while the bandwidth was less than 1%. The IR beam was focused through a 2 mm thick zinc selenide window into the center of the ion trap with a 60 cm focal length zinc selenide lens.

Vanadium oxide clusters are prepared by pulsed laser vaporization with the second harmonic (532 nm, 8 ns, ∼10 mJ pulse^{-1} at 20 Hz) of a Nd : YAG laser focused onto a rotating and translating 6 mm diameter solid vanadium rod (Alfa Aesar, 99.5% purity). The resulting plasma is entrained in a pulse of 1% O_2 seeded in He carrier gas, expanded through a clustering channel and passed through a 2 mm skimmer.

Positive ions are focused into a radio frequency (RF) quadrupole ion guide (Q_0 in Fig. 1), which collimates the ion beam, then deflected by 90° by the quadrupole ion deflector D_0 into the first RF quadrupole mass filter Q_1, which is typically operated at unit resolution. Mass-selected ions are guided *via* the second 90° deflector D_1 and two sets of einzel lenses (E_1 and E_2) into a temperature-adjustable, He filled RF hexadecapole ion guide (H). The arrangement of a gas-filled RF ion guide in-between two electrostatic lenses can be used as an efficient ion trap.[31] Ions entering the trap, which is connected to a helium cryostat and kept at a constant temperature of < 70 K, lose both kinetic and internal energy due to inelastic collisions with the cooled He buffer gas (∼0.08 mbar). Applying appropriate electrostatic potentials to the entrance lens, ion guide pole bias voltage and exit lens of the trap allows ions to be trapped over a period of seconds, effectively increasing the ion density inside the trap and thermalizing the trapped ions to the ambient temperature on a timescale of roughly 10^{-4} s.[32]

Trapping conditions were optimized on the ion signal and with respect to signal-to-background considerations. In the present experiment the ion trap is continuously filled for a period of 1 s. During this time on average five FELIX macro pulses, which are applied collinearly to the trap axis, pass through the ion trap. When FELIX is tuned in resonance with an allowed IR transition, cluster ions may absorb one or more photons (provided that internal relaxation occurs rapidly compared to the FELIX micro pulse spacing of 1 ns). If the internal energy has risen sufficiently, the ion will dissociate. The fragment ion will remain confined in the trap. To extract ions a 5 ms extraction pulse is applied to the ion trap exit lens. Extracted ions are guided into the second RF quadrupole mass filter Q_2. The yield of mass-selected product ions is monitored by a subsequent off-axis conversion dynode channeltron detector (Det) operated in the pulse counting mode.

At each wavelength 10 fill/extraction cycles (15 for the higher resolution spectra) are performed and the total frag-
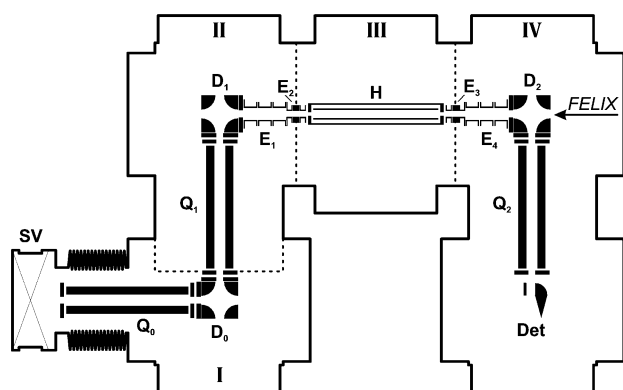
ment ion count is saved. Before and after detection of the fragment ion signal, the intensity of the parent ion signal is monitored. The yield of fragment ions as a function of FELIX wavelength then yields the photodissociation spectrum.

A typical mass spectrum of vanadium oxide cluster cations produced by laser vaporization with 1% O_2 seeded in He carrier gas is shown in Fig. 2. Vanadium oxide clusters ranging from $V_2O_4^+$ to $V_8O_{20}^+$ are observed. With the exception of $V_5O_{14}^+$, which is produced with a much lower yield than expected, the intensity distribution within each $V_xO_y^+$, $V_xO_{y+1}^+$, ... series varies smoothly with cluster size. The present source conditions favor the generation of oxygen-rich $V_xO_y^+$ clusters. For a given number of vanadium atoms the most intense peak in the mass spectrum is found at a vanadium to oxygen ratio of roughly 1 : 2.4. The mass spectrum is in
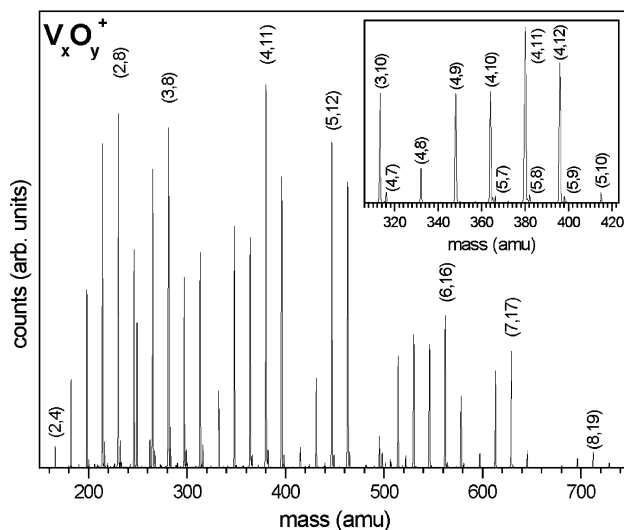

Fig. 2 Mass spectrum of vanadium oxide cluster cations $V_xO_y^+$ produced by pulsed laser vaporization using a gas mixture of 1% O_2 seeded in helium carrier gas. Selected peaks are labeled with numbers in parentheses, (*x*,*y*), denoting the cluster composition. The mass region from 310 to 425 amu is shown enlarged in the top right corner.
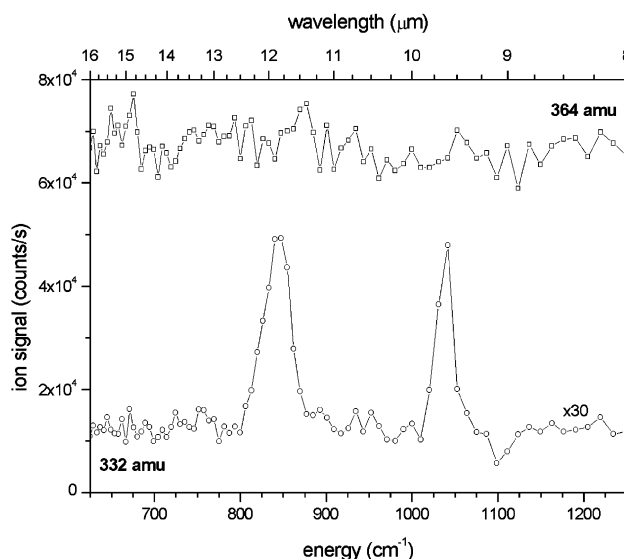

Fig. 1 Schematic of the guided ion beam tandem mass spectrometer (see text for details). D_{0-2}: electrostatic 90° quadrupole deflectors; Det: conversion dynode channeltron detector; E_{1-4}: einzel lenses; GV: gate valve; H: RF hexadecapole ion trap; Q_0: RF quadrupole ion guide; $Q_{1,3}$: RF quadrupole mass filters.

Fig. 3 Gas-phase IR photodissociation spectra of $V_4O_{10}^+$ in the spectral region from 8 to 16 μm (1250 to 625 cm^{-1}) scanned in steps of 0.1 μm. Parent ion spectrum (364 amu. top trace) and $V_4O_8^+$ fragment ion spectrum (332 amu, bottom trace), corresponding to loss of O_2, are plotted as a function of FELIX wavelength (top axis) and energy (bottom axis).

good agreement with recently published mass spectra, which were measured using a similar cluster ion source, but with a ten times higher O_2 content in the carrier gas.[8]

The IR photodissociation spectrum of mass selected $V_4O_{10}^+$ (364 amu) in the range from 625 to 1250 cm^{-1} is shown in Fig. 3 (bottom trace). It was measured by mass selectively monitoring the $V_4O_8^+$ (332 amu) fragment ion yield as a function of FELIX wavelength, after irradiating $V_4O_{10}^+$ ions confined in the ion trap. The signal of unfragmented parent ions is also shown (top trace). It varies by roughly ±10% over a time of 30 min, the aquisition time of the depicted spectra, and reflects minor changes in the source conditions as a function of time. Depletion of the parent ion signal, which is on the order of 3% at the maximum fragment ion signal, is masked by these variations. The fragment ion signal is comprised of two parts. The constant background signal results from dissociation induced by collisions with the He atoms as the ions enter the trap. Superimposed on this constant background signal due to photoinduced dissociation is observed. The spectrum shows two peaks at 9.6 and 11.8 μm. Tuning FELIX to these resonant frequencies and scanning the second mass filter revealed no fragmentation channels other than the loss of O_2 (or loss of two O atoms, which cannot be discerned using the present experimental setup).

Higher resolution spectra measured with smaller wavelength step size, longer dwell times and in a narrower wavelength region are shown in Fig. 4. These spectra were corrected for variations in the parent ion signal, by scaling the parent ion spectrum by a factor of 0.03 and subtracting it from the corresponding fragment ion signal. The two observed peaks have nearly Lorentzian shapes and an appropriate least square fit yields peak maxima and peak widths (full width at half maximum) of 842 cm^{-1} (32 cm^{-1}) and 1032 cm^{-1} (9 cm^{-1}). The width of the first peak is substantially larger than the bandwidth of FELIX, which was roughly < 1% in the present study. Based on calculations of Vyboishchikov et al.[23] on the IR spectroscopy of neutral V_4O_{10} isomers we assign the 842 cm^{-1} and 1032 cm^{-1} features to the antisymmetric V–O–V stretching and the V=O stretching vibrations, respectively.
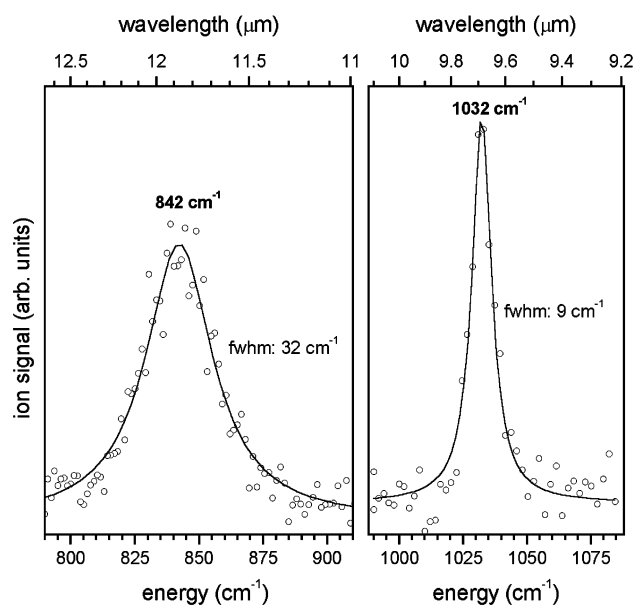

Fig. 4 Gas-phase IR photodissociation spectra (solid dots) of $V_4O_{10}^+$ measured by monitoring the $V_4O_8^+$ fragment ion signal (O_2 loss). The spectra were measured in steps of 0.02 μm and corrected for fluctuations in the parent ion signal (see text). Peak maxima and widths were determined by fitting a Lorentz function to the experimental data (solid line).

For various neutral isomers these are calculated to lie in-between 800–925 cm^{-1} (V–O–V stretch) and 1040–1080 cm^{-1} (V=O stretch).

We first address the observed fragmentation behavior with respect to the photofragmentation mechanism and then discuss the structure of the $V_4O_{10}^+$ cation. Fragmentation of $V_4O_{10}^+$ has previously been studied by CID and photofragmentation using 532 nm radiation.[7,8] Single collisions with Xenon atoms lead to O_2 loss already at thermal energies, while other fragmentation channels are only observed at collision energies above 3 eV. Similarly, absorption of a single 532 nm (2.128 eV) photon leads exclusively to O_2 loss, while other fragmentation channels are only observed at higher laser fluences, i.e., under multi-photon absorption conditions. Based on these results it is inferred that $V_4O_{10}^+$ is composed of an O_2 molecule weakly attached to a strongly bound $V_4O_8^+$ ion core. It is difficult to estimate an upper limit for the dissociation energy of the O_2 loss channel from these experiments, as the cluster internal temperature is not known.

Evidence for a weakly bound $V_4O_8^+ \cdot O_2$ complex is also found in the present study. Cluster ions formed by standard laser vaporization sources are generally "hot" and their internal temperature is often controlled by an evaporative cooling mechanism, i.e., the internal energy is close to but less than the energy required to break the weakest bond in the system. Such internally "hot" clusters can dissociate upon entering the He filled ion trap. The initial collisions with the He atoms determine the fate of these cluster ions. Either they dissociate within the first few collisions or they are cooled down to the ambient temperature (< 70 K), at which point fragmentation by collisions with He atoms has been effectively quenched. This accounts for the constant background signal observed.

Because the (lowest) dissociation energy of $V_4O_{10}^+$ is unknown, it is difficult to estimate the minimum number of absorbed photons required to induce photofragmentation. For the single photon absorption case, fragmentation occurs at the fundamental vibrational frequencies of the parent ion. Under the present power and fluence conditions also multiple photons can be absorbed. A *coherent stepwise* multiphoton absorption mechanism is, however, unrealistic, due to the "anharmonic bottleneck" of a vibrational potential.[29] Resonant excitation by multiple photons rather proceeds *via* a *sequential incoherent* absorption mechanism particular to the pulse structure of free electron lasers. After absorption of a single photon (or a few photons) rapid intramolecular vibrational energy redistribution (IVR) efficiently de-excites the absorbing vibrational state within less than ~1 ns, allowing subsequent photons to be absorbed. Note, quenching of the absorption due to collisions with the He buffer gas is negligible in the present experiment, due to the considerably larger time scale for thermalization (to the ambient temperature) compared to IVR. With an increasing number of absorbed photons this mechanism will lead to a distortion and a red shift of the spectral features.[33] Taking into account the symmetric band shapes and the absence of any other fragmentation products we assume that not more than a few photons are required to induce fragmentation of $V_4O_{10}^+$, which supports the proposed, weakly-bound $V_4O_8^+ \cdot O_2$ structure. The width of the 1032 cm^{-1} band is on the order of the laser bandwidth. The three times larger width of the 842 cm^{-1} band is surprising. It could in principle result from lifetime broadening ($\tau \approx 170$ fs) and indicate a mode dependent, efficient vibrational predissociation mechanism or simply be the result of multiple overlapping bands. This aspect warrants further study in the future.

Determination of the structure of $V_4O_{10}^+$ can also be aided by comparison of the present data with the results from a recent density functional theory study on the IR spectroscopy of various isomers of neutral V_4O_{10}.[23] On the basis of these results we have already assigned the observed peaks to the

antisymmetric V–O–V stretching and terminal V=O stretching vibrations. All calculated isomers show absorption in this spectral region. Best agreement between calculated and experimental spectra is found for the highly symmetric cage structure (labeled TETRA in ref. 23), namely due to the absence of strong absorption at longer wavelengths for this isomer. The other three isomers, which were derived from bulk-like crystalline structures of V_2O_5, show additional absorption features of similar intensity at energies below 800 cm^{-1}, characteristic for V–(O)$_2$–V double bridges. No fragmentation is detected in the 625–800 cm^{-1} region in the present study. The calculated cage-like structure is the lowest energy structure of all four isomers considered. It, however, lacks a weakly bound O_2 unit and therefore it is not straightforward to account for the observed fragmentation behavior assuming such a structure. We tentatively conclude that the absorbing species consists of a $V_4O_8^+$ ionic core, which lacks any V–(O)$_2$–V double bridges, and is weakly bound to an oxygen molecule.

It might be possible that other more strongly bound isomers of $V_4O_{10}^+$ are present in the ion trap, but do not dissociate under the present experimental conditions and thus are not detected. We presently have no means to check this, nor do the theoretical studies treat the energetics of the weakly bound complex. Assuming only a weak perturbation of the $V_4O_8^+$ structure by the presence of O_2, it may, however, be more reasonable to state that we are probing the most stable $V_4O_8^+$ (rather than $V_4O_{10}^+$) isomer, since this $V_4O_8^+$ isomer should intuitively also lead to the most abundant formation of $V_4O_8^+ \cdot O_2$. We are currently improving the experimental setup to generate a larger flux of photons at the interaction region in order to reach energetically higher lying fragmentation channels. This is in principle possible, as the recent study on cationic polyaromatic hydrocarbons has shown, where dissociation energies of more than 6 eV were overcome.[29]

We conclude by highlighting several aspects of the presented experimental technique, which we believe, make it generally applicable. (a) The technique is not limited to the study of a particular species, but may be applied to a wide variety of ions that can be generated with various cluster ion sources available today. (b) Presently, the technique is limited to ions with moderately low dissociation energies (smaller ~1–2 eV), but more strongly bound clusters can be studied, by adding a weakly bound "spectator" atom or molecule to the cluster ion. (c) It yields IR spectra of cooled, mass-selected cluster ions in a spectral region, which should allow for a unique structural characterization of many cluster ions of interest based on the comparison between experimentally and theoretically determined vibrational frequencies.

References

1 C. N. R. Rao and B. Raven, *Transition Metal Oxides*, VCH Press, New York, 1995.
2 D. Yin, N. Xu, J. Zhang and X. Zheng, *J. Phys. D*, 1996, **29**, 1051.
3 B. Grzybowska-Swierkosz, *Appl. Catal. A*, 1997, **157**, 263.
4 H. Wu and L.-S. Wang, *J. Chem. Phys.*, 1998, **108**, 5310.
5 L. B. Knight Jr., R. Babb, M. Ray, T. J. Banisaukas III, L. Russon, R. S. Dailey and E. R. Davidson, *J. Chem. Phys.*, 1996, **105**, 10 237.
6 G. V. Chertihin, W. D. Bare and L. Andrews, *J. Phys. Chem. A*, 1997, **101**, 5090.
7 S. E. Kooi and A. W. Castleman Jr., *J. Phys. Chem. A*, 1999, **103**, 5671.
8 R. C. Bell, K. A. Zemski, K. P. Kerns, H. T. Deng and A. W. Castlemann Jr., *J. Phys. Chem. A*, 1998, **102**, 1733.
9 R. C. Bell, K. A. Zemski and A. W. Castleman Jr., *J. Phys. Chem. A*, 1998, **102**, 8293.
10 R. C. Bell, K. A. Zemski and A. W. Castleman Jr., *J. Phys. Chem. A*, 1999, **103**, 2992.
11 R. C. Bell, K. A. Zemski and A. W. Castleman Jr., *J. Phys. Chem. A*, 1999, **103**, 1585.
12 R. C. Bell, K. A. Zemski, D. R. Justes and A. W. Castleman Jr., *J. Chem. Phys.*, 2001, **114**, 798.
13 A. Dinca, T. P. Davis, K. J. Fisher, D. R. Smith and G. D. Willett, *Int. J. Mass Spectrom. Ion Processes*, 1999, **182/183**, 73.
14 J. N. Harvey, M. Diefenbach, D. Schröder and H. Schwarz, *Int. J. Mass Spectrom. Ion Processes*, 1999, **182/183**, 85.
15 E. B. Rudnyi, E. A. Kaibicheva and L. N. Sidorov, *J. Chem. Thermodyn.*, 1993, **25**, 929.
16 A. Fielicke and K. Rademann, *Phys. Chem. Chem. Phys.*, 2001, submitted (B108046F).
17 K. A. Zemski, D. R. Justes and A. W. Castleman Jr., *J. Phys. Chem. A*, 2001, **105**, 10 237.
18 G. C. Nieman, E. K. Parks, S. C. Richtmeier, K. Liu, L. G. Pobo and S. J. Riley, *High. Temp. Sci.*, 1986, **22**, 115.
19 M. Foltin, G. J. Stueber and E. R. Bernstein, *J. Chem. Phys.*, 1999, **111**, 9577.
20 L. Karlsson, B. Lindgren, C. Lundevall and U. Sassenberg, *J. Mol. Spectrom.*, 1997, **181**, 274.
21 J. Brett, *Astron. Astrophys.*, 1990, **231**, 440.
22 S. F. Vyboishchikov and J. Sauer, *J. Phys. Chem. A*, 2000, **104**, 10 913.
23 S. F. Vyboishchikov and J. Sauer, *J. Phys. Chem. A*, 2001, **105**, 8588.
24 M. Calatayud, B. Silvi, J. Andrés and A. Beltrán, *Chem. Phys. Lett.*, 2001, **333**, 493.
25 H. D. Babcock and L. Herzberg, *Astrophys. J.*, 1948, **108**, 167.
26 M. A. Duncan, *Int. J. Mass Spectrom.*, 2000, **200**, 545.
27 G. von Helden, I. Holleman, G. M. H. Knippels, A. F. G. van der Meer and G. Meijer, *Phys. Rev. Lett.*, 1997, **79**, 5234.
28 H. Piest, G. von Helden and G. Meijer, *J. Chem. Phys.*, 1999, **110**, 2010.
29 J. Oomens, A. J. A. van Roij, G. Meijer and G. von Helden, *Astrophys. J.*, 2000, **542**, 404.
30 D. Oepts, A. F. G. van der Meer and P. W. van Amersfoort, *Infrared Phys. Technol.*, 1995, **36**, 297.
31 G. G. Dolnikowski, M. J. Kristo, C. G. Enke and J. T. Watson, *Int. J. Mass Spectrom. Ion Processes*, 1988, **82**, 1.
32 J. Westergren, H. Grönbeck, S.-G. Kim and D. Tománek, *J. Chem. Phys.*, 1997, **107**, 3071.
33 G. von Helden, I. Holleman, G. Meijer and B. Sartakov, *Opt. Express*, 1999, **4**, 46.